# Bent metallocenes revisited

**Jennifer C. Green**

*Inorganic Chemistry Laboratory, South Parks Road, Oxford UK OX1 3QR*

CHEMICAL SOCIETY REVIEWS

**The orbital structure of bent metallocenes and how their geometry depends on the number of d electrons are described. Bonding by a metallocene unit is exemplified by reference to the known hydrides. The reactivity of metallocene derivatives is illustrated with particular emphasis on the differences between *ansa*-bridged and unbridged compounds; the reactions include ring opening polymerisation of ferrocenophanes, elimination from and addition to Group 6 metallocene derivatives and Ziegler–Natta polymerisation of olefins by Group 4 metallocenes.**

## 1 Introduction

Shortly after the discovery of ferrocene and the establishment of its sandwich structure, with parallel rings, **I**, came the discovery that bis-cyclopentadienyl metal complexes could be synthesised in which the two $C_5$-rings are inclined at an angle to one another and there are also additional ligands attached to the metal, **II**.[1]

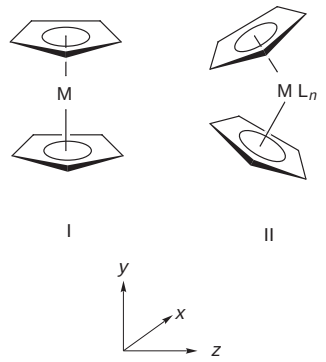


The high symmetry of ferrocene and its first row transition metal analogues enabled qualitative molecular orbital methods to be applied successfully to describe its bonding with a high degree of confidence. Ligand field theory was used to treat the d electrons and rationalise spectroscopic and magnetic properties. The lower symmetry bent metallocenes were less tractable,[2] but physical studies[3–5] and semi-empirical theoretical treatments[6,7] produced a coherent model describing the orbital structure of these species which has been invaluable in interpreting the wide variety of basic chemical processes in which these bent metallocenes participate.

The study of bent metallocenes has generated a wealth of chemistry which has demonstrated and led to understanding of many fundamental transformations; for example for the tungstenocene system these include photochemical reductive elimination of dihydrogen, insertion of $Cp_2W$ [Cp = ($\eta$-$C_5H_5$)] into saturated $sp^3$ C–H bonds, first evidence for reversible α-H elimination, and development of rules for predicting the regioselectivity of nucleophilic addition to organometallic cations.[8]

In recent years metallocenes have become of considerable commercial importance providing, in combination with methyl alumoxane, a new generation of Ziegler–Natta type polymerisation catalysts for production of polyethylene and polypropylene.[9–11]

The aim of this article is to review the bonding model for bent metallocenes and to show how their orbital structure relates to some of the unusual reactivity shown by these compounds. The selection of material is eclectic rather than comprehensive.

In Fig. 1 the various structural parameters used in this review are defined for a bent metallocene unit (a) and for an *ansa*-bridged metallocene unit (b).

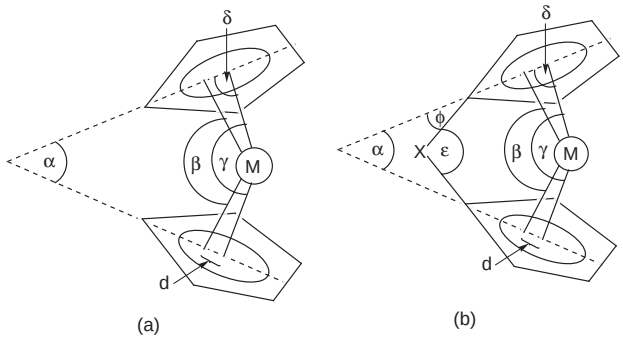


**Fig. 1** Geometric parameters in a bent metallocene: $\alpha$ = angle between the ring planes; $\beta$ = angle between the normals from the metal to the ring planes; $\gamma$ = ring centroid-metal-ring centroid angle; $\delta$ = angle between the ring plane and the metal-ring centroid vector; $\varepsilon$ = angle between the vectors from a bridging atom X to the *ipso*-carbons; $\phi$ = angle between the *ipso*-carbon vector and the ring plane; d = the ring slippage, the displacement of the ring centroid from the normal to the ring plane.

There is generally found to be little departure from planarity of the cyclopentadienyl rings. The angle between the rings is normally defined in one of three ways, either as $\alpha$, the angle between the ring planes, or $\beta$, the angle between the metal-ring normals ($\alpha + \beta = 180°$) or $\gamma$, the angle between the vectors from the metal to the ring centroids. When the rings are linked by a bridge X, $\varepsilon$ gives the angle at the bridging atom and $\phi$ the angle between the ring plane and the vector from the *ipso*-carbon to the bridging atom.

*Jennifer Green gained her BA, MA and DPhil at the University of Oxford, the latter under supervision of Jack Linnett and Peter Atkins. She then held a Turner and Newall Research Fellowship after which she was appointed a Fellow and Tutor in Chemistry at St Hugh's College. Her current position is that of University Reader in the Inorganic Chemistry Laboratory. Her research has focused on the electronic structure of transition metal compounds which she has investigated both theoretically and experimentally using photoelectron spectroscopy.*

## 2 MO model for a bent metallocene unit

The orbital structure of ferrocene is well established; a schematic energy level diagram is given in Fig. 2. The top four occupied energy levels are also illustrated in Fig. 3. In $D_{5h}$ symmetry† the top three occupied orbitals are to a first approximation non-bonding and principally metal 3d in character. The $d_{z2}$ orbital has minimal overlap with the ring pπ orbitals as its nodal cone intersects the region of maximum electron density of these orbitals. It is the major contributor to the $a_1'$ orbital where it is mixed with the 4s orbital and avoids a ligand contribution. The $d_{x2-y2}$ and $d_{xy}$ orbitals have the potential to back-bond into the empty ring orbitals of $e_2'$ symmetry but as these are rather high in energy the back bonding contribution is small. The principal bonding interaction is between the metal $d_{xz}$ and metal $d_{yz}$ orbitals and the ring $e_1''$ π orbitals. The $e_1'$ combinations of ring π orbitals are less effective at bonding as they can only combine with the metal p orbitals and these are high in energy. Similarly the mixing between the ring $a_1'$ π orbitals and the metal s orbital is much more effective than that between the ring $a_2''$ π combination and the metal $p_z$ orbital. Thus as a consequence of the high symmetry of ferrocene only three of the molecular orbitals have significant metal ligand bonding characteristics.

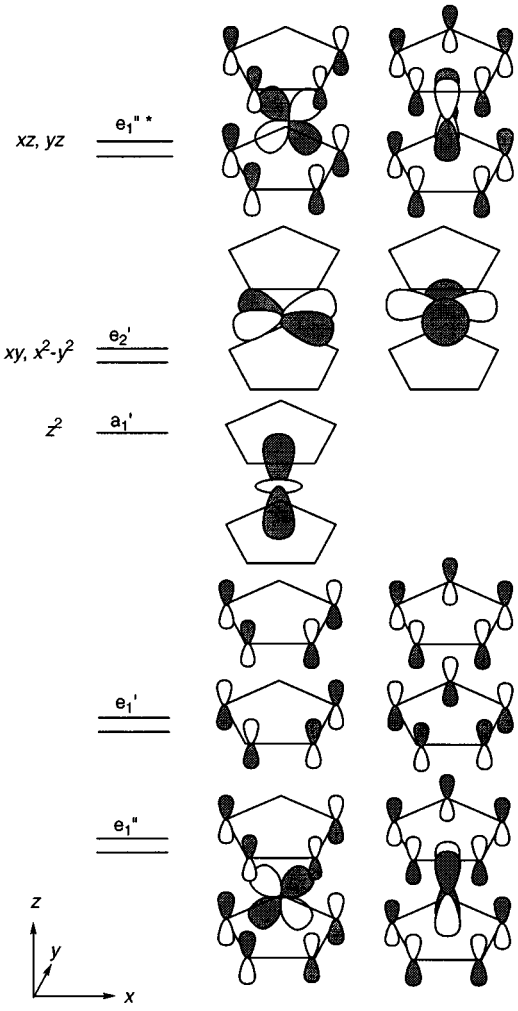


**Fig. 2** Schematic energy level diagram for a $D_{5h}$ metallocene; for ferrocene the levels are occupied up to the $e_2'$ orbitals and the antibonding $e_1''$* orbital is empty

The changes in the wave functions which occur when the molecule is bent with $\alpha = 35°$ are illustrated in Fig. 3. Fig. 4 gives the variation of one electron energies as a function of angle, $\alpha$. Lowering the symmetry from $D_{5h}$ to $C_{2v}$‡ causes two of the three occupied d orbitals to become the same symmetry, $a_1$; as the molecule bends they mix and move apart in energy, the upper one, $4a_1$, becoming less stable and the lower one, $3a_1$, eventually more stable. The third d orbital becomes $b_1$ in symmetry and increases in energy though not as much as the $4a_1$ orbital. Both the $4a_1$ and $2b_1$ orbitals are directed towards the open side of the metallocene wedge. These two orbitals have greater amplitude towards the open side of the wedge. As the rings are bent, destructive interference between the metal d-orbitals and the ring pπ orbitals where the rings approach each other leads to this asymmetry in electron distribution and the outward pointing direction of these orbitals. The $3a_1$ orbital resembles a $d_{x2}$ orbital pointing along the *x* axis. All three orbitals have their maximum probability density in the *xz* plane.

Removal of the symmetry constraint also affects the top occupied cyclopentadienyl orbitals. In the lower symmetry all four symmetry adapted linear combinations can interact with the metal d orbitals. The $e_1'$ orbitals become the $2a_1$ and $1b_1$ orbitals and drop in energy on bending becoming bonding rather than non-bonding. The drop in energy of these two orbitals is more or less mirrored by the rise in energy of the $4a_1$ and $2b_1$ orbitals. Of the $e_1''$ orbitals, one becomes $b_2$ in symmetry, loses overlap with the metal orbitals and is raised in energy on bending; the other, the $1a_2$ orbital, remains almost constant in energy.

The increase in the number of bonding interactions on bending suggests that bent structures might well be favourable, however it is well established that all the isolated transition metal metallocenes have a parallel sandwich structure. Bent structures are favoured by the $d^0$ pre-transition metals Ca, Sr and Ba,[12] though, as the bonding forces involved with these elements are more electrostatic than covalent, calculations show the structural preference to be slight. However, there is a good case for believing that it is the d orbital occupancy that controls the angle between the rings of a metallocene.

Fig. 5 shows how the calculated total energy of both ferrocene and the hypothetical triplet zirconocene vary with $\alpha$. When all three d orbitals are fully occupied as in ferrocene the total energy of the molecule is raised significantly in energy on bending. However when the $4a_1$ orbital is unoccupied as in zirconocene with the configuration $3a_1^1\ 2b_1^1$, the overall energy drops slightly. Thus ferrocene shows a strong preference for a parallel ring arrangement whereas the hypothetical moiety $ZrCp_2$ would show little resistance to angle variation.

Further theoretical investigation of the optimised structures of 4d metallocenes shows a definite pattern (Table 1).§ If the $4a_1$ orbital is occupied, parallel or nearly parallel ring structures result, but if it is unoccupied a bent structure with $\alpha > 30°$ is favoured. The small deviation from planarity for triplet $MoCp_2$ and $TcCp_2$ is expected on the basis of the Jahn–Teller theorem,

† Ferrocene is known to have rapidly rotating rings even in the solid state. The energy barrier to ring rotation is estimated to be 5–10 kJ $mol^{-1}$. At low temperatures the relative orientation of the rings is closer to eclipsed than staggered. It is convenient for the purposes of this article to assume the $D_{5h}$ symmetry consistent with an eclipsed structure. The symmetry labels for the MO of ferrocene will thus differ from those found in most text books where $D_{5d}$ symmetry is assumed, however, the essential details of the bonding are the same.

‡ The highest possible symmetry for a bent metallocene unit is $C_{2v}$. The axis system we assume throughout this article is shown in Fig. 1. Although there is universal agreement that the $C_{2v}$ axis lies in the *z* direction, different choices of *x* and *y* axes lead to different labels for orbitals in a $C_{2v}$ molecule, so care must always be taken when comparing results from different studies. $C_{2v}$ is conveniently a sub group of $D_{5h}$ so we can correlate the orbitals of a parallel and a bent metallocene. Our choice of axes means that the $\sigma_h$ of the $D_{5h}$ molecule becomes the *xz* plane in $C_{2v}$ symmetry.

§ The results presented here are from density functional calculations using the Amsterdam Density Functional code, ADF 2.0.1 Baerends and te Velde Vreije Universiteit Amsterdam 1996.

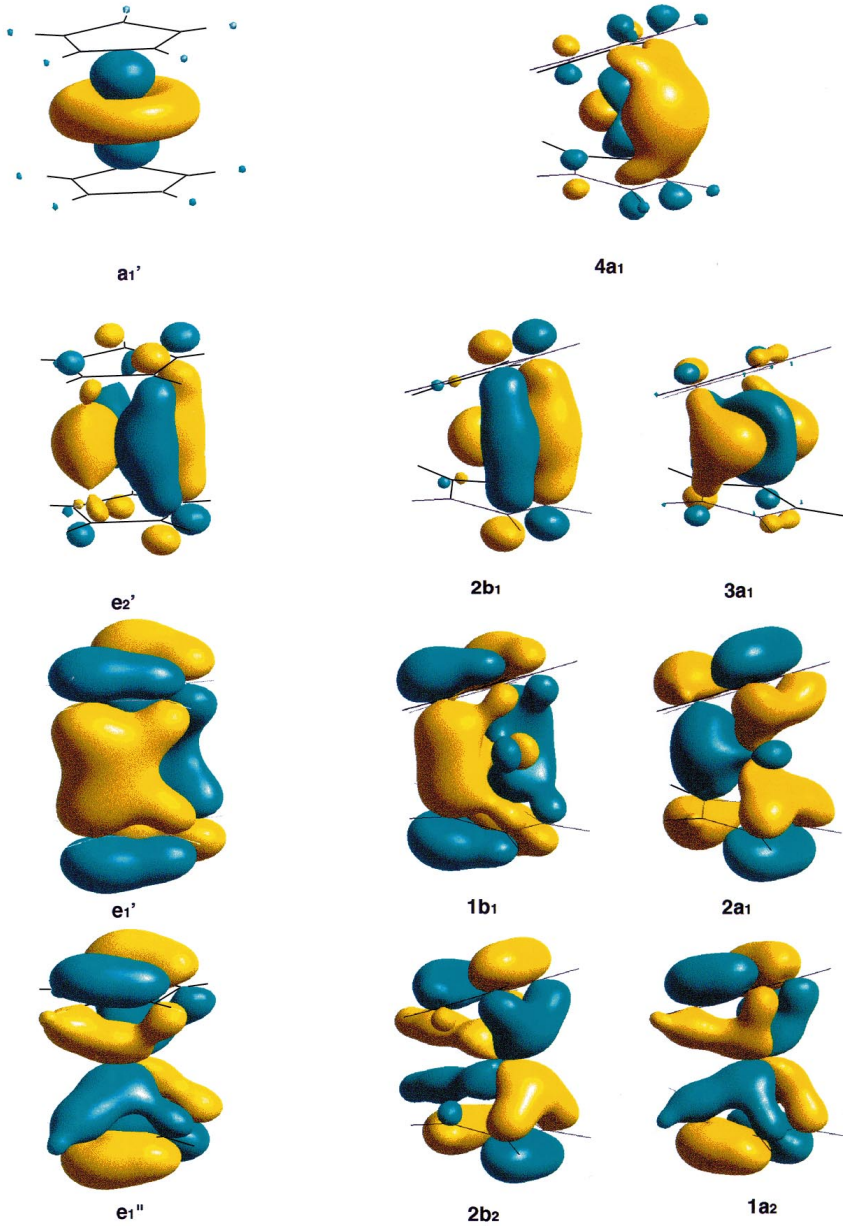


**Fig. 3** Isosurfaces for the orbitals of a bent metallocene unit. (These were generated using the Cerius² package of Molecular Simulations Inc.)

indeed matrix isolated molybdenocene has been shown to be bent.[13] Tungstenocene has a parallel sandwich structure as spin orbit coupling suppresses the Jahn–Teller distortion. $TiCp^*_2$ [Cp* = ($\eta$-$C_5Me_5$)],[14] a $d^2$ metallocene, has not been structurally characterised but may well be bent.

**Table 1** Optimised bending angles and average metal–carbon distances for the second row metallocenes.

| Metal | Configuration | Spin state | $\alpha$° | M–C av/Å | Energy (eV) |
|---|---|---|---|---|---|
| Y | $3a_1^1 2b_1^0 4a_1^0$ | doublet | 40.9 | 2.62 | −124.59 |
| Zr | $3a_1^1 2b_1^1 4a_1^0$ | triplet | 36.3 | 2.49 | −125.96 |
| Zr | $3a_1^2 2b_1^0 4a_1^0$ | singlet | 47.8 | 2.46 | −125.74 |
| Nb | $3a_1^1 2b_1^1 4a_1^1$ | quartet | 0 | 2.43 | −127.63 |
| Nb | $3a_1^2 2b_1^1 4a_1^0$ | doublet | 40.5 | 2.37 | −126.79 |
| Mo | $3a_1^2 2b_1^1 4a_1^1$ | triplet | 18.4 | 2.33 | −127.28 |
| Mo | $3a_1^2 2b_1^2 4a_1^0$ | singlet | 35.3 | 2.29 | −126.48 |
| Tc | $3a_1^2 2b_1^2 4a_1^1$ | doublet | 11.2 | 2.26 | −128.36 |
| Ru | $3a_1^2 2b_1^2 4a_1^2$ | singlet | 0 | 2.21 | −126.74 |

Where two states with differing spins are possible the lower energy state is that of maximum multiplicity, but the average metal–carbon distance tends to be shorter in the low spin bent structures. The preference for the maximum number of unpaired electrons will be greater in the first transition series where exchange interactions are stronger and ligand field splittings less.

In conclusion, it is the d electron configuration that controls the geometry of the transition metal metallocenes. The commonly found parallel ring structures are a consequence of the d electrons avoiding anti-bonding interactions and minimising electron–electron repulsion. In the absence of these forces there is no inherent weakening of the metal ring bonding on bending.

## 3 Further bonding by a metallocene unit

The $3a_1$, $2b_1$ and $4a_1$ orbitals of a bent metallocene constitute the three frontier orbitals which can be used to bind further ligands. The simplest example of this is the formation of the hydrides $MCp_2H$, III (M = Re), $MCp_2H_2$, IV (M = Mo, W) and $MCp_2H_3$, V (M = Nb, Ta). In all cases the hydride ligands lie in the *xz* plane of the metallocene unit.

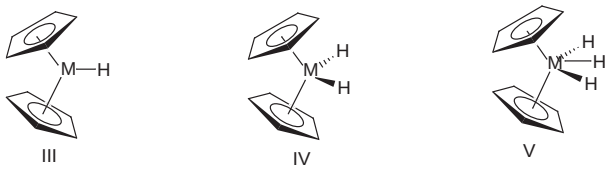


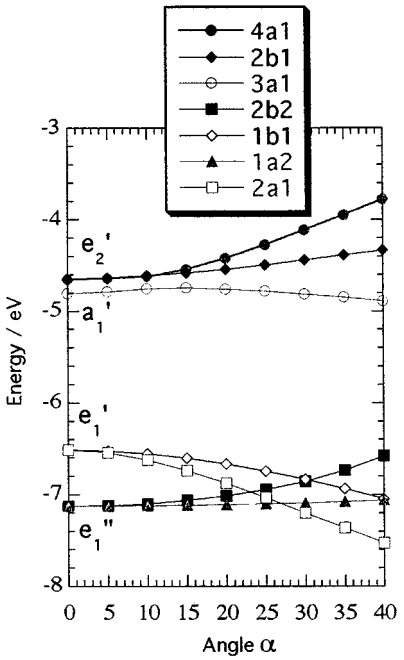


**Fig. 4** Variation of one electron energies of ferrocene as a function of bending angle $\alpha$

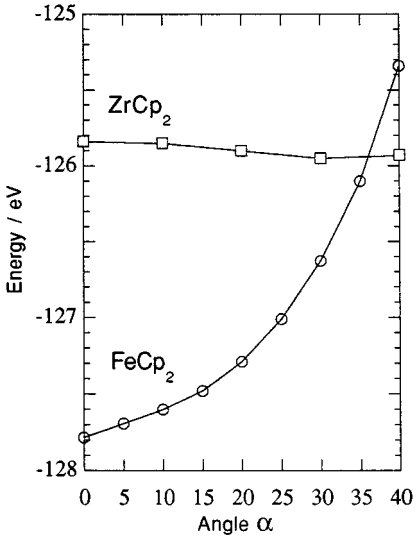


**Fig. 5** Variation of total energy of ferrocene and triplet zirconocene as a function of bending angle $\alpha$

In each case the metallocene unit provides a symmetry match to the symmetry adapted linear combinations (SALCs) of the hydrogens' 1s orbitals (Fig. 6). **III**, with one M–H bond, has a $d^4$ configuration with two lone pairs of $a_1$ and $b_1$ symmetry. **IV** has one lone pair of $a_1$ symmetry and **V** none. Photoelectron studies of these compounds clearly show the high lying lone pairs which have low ionisation energies (IEs). The M–H bonding electrons have IEs of similar magnitude to the top occupied cyclopentadienyl orbitals.[4]

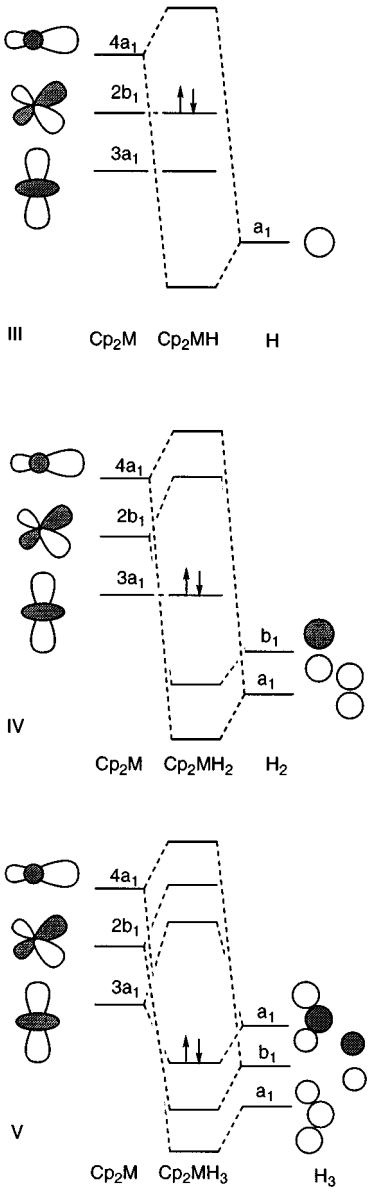


**Fig. 6** MO schemes for binding $H_{1\text{-}3}$ to $MCp_2$ to give **III**, **IV** and **V**. The orbitals are drawn as projections on the *xz* plane. The HOMOs of **III**, **IV** and **V** are denoted by a double arrow.

There is good physical evidence for the spatial location of the $a_1$ HOMO in a compound with the stoichiometry $MCp_2X_2$. In the series where X = Cl and M = Zr, Nb and Mo the compounds have the configuration $d^0$, $d^1$ and $d^2$ respectively. The Cl–M–Cl angle decreases along the series, 97.1° (Zr), 85.6° (Nb) and 82.0° (Mo).[3] The presence of electrons in a $d_{x^2}$ like orbital causes the Cl–M–Cl angle to close up. In $MoCp_2H_2$ the H–Mo–H angle is 75.5°.[15] Thus **VI** provides a better picture of the lone pair in a metallocene than does **VII**. An ESR study of a number of $d^1$ compounds shows the half-occupied $a_1$ orbital to consist mainly of $d_{x^2}$ with a small admixture of $d_{y^2-z^2}$.[5]

In the trihydride $TaCp_2H_3$ the H–Ta–H angles are 63° and the adjacent H–H distance is 1.85 Å.[16] Such close approach is unfavourable for larger ligands, and there are no structurally characterised examples of metallocene units bound to three monodentate ligands other than hydrogen.

Both $NbCp_2H_3$ and $[MoCp_2H_3]^+$ show an $^1H$ NMR spectrum in a certain temperature regime consistent with an $AB_2$ spin system but with unusually large $J_{AB}$ coupling constants; that of the Nb compound is 20.4 Hz above 243 K while that of the Mo compound varies from *ca.* 1000 Hz at 203 K to 450 Hz at 153 K.[17] Such a massive value is due to quantum mechanical

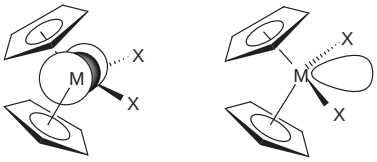


VI VII

exchange coupling. It has been argued that the the main factor governing the magnitude of the exchange coupling is the stability of an $[MCp_2(\eta\text{-}H_2)H]^{n+}$ structure, **VIII**, relative to the minimum energy trihydride.[18] However, Heinekey[19] maintains that the formation of an $H_2$ intermediate is not required, but that a large quantum mechanical exchange coupling is favoured by a soft vibrational potential for the $WH_AH_B$ wag. A low frequency for this motion allows close approach of the hydrogens and substantial overlap of the hydride wave functions leading to the observed tunnelling.

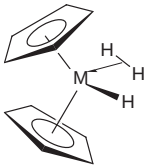


VIII

Deuteration of the $d^2$ hydride $WCp^*_2H_2$ to form the cation $[WCp^*_2H_2D]^+$ occurs preferentially between the two hydrogens (1) giving 90% of the central isotopomer (1a) rather than the lateral one (1b),[20] which would be expected by direct protonation of the occupied $3a_1$ orbital. Attack is at the hydride ligands and is subject to charge rather than orbital control. Subsequent exchange between the central and lateral positions is found to occur at a faster rate than deprotonation and further deuteration demonstrating the presence of an intramolecular exchange mechanism. Kinetic studies on protonation of $WCp_2H_2$ suggests the presence of the intermediate $[WCp_2(\eta^2\text{-}H_2)H]^+$ in the protonation reaction.[21]

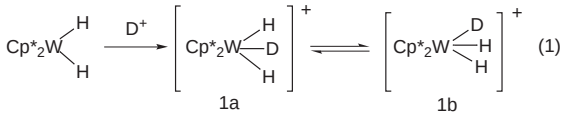


1a 1b

Several other bonding situations for the versatile bent metallocene unit are discussed by Lauher and Hoffmann.[7] A case not explicitly considered there is the bonding of a metallocene unit to an imido group, to form $MoCp_2NR$ complexes. The $NR^{2-}$ ligand is a strong π donor and therefore has the capacity to form a triple bond to a transition metal. A metallocene fragment readily provides only one acceptor π orbital, the $2b_1$ orbital in the *xz* plane. The $d_{yz}$ orbital is involved in bonding to the rings in the $2b_2$ orbital. The anti-bonding counterpart, $3b_2$, descends in energy on bending but lies some 1.5 eV above the $4a_1$ orbital. It may be considered as a fourth frontier orbital of the $MCp_2$ unit (Fig. 6). In the compound $MoCp_2NBu^t$ the Mo–N–C angle is 177.7° indicating that both N pπ orbitals are interacting with the metal, and the Mo–N distance is consistent with a bond order between 2 and 3; both factors suggest a $b_2$ Mo–N π bonding interaction.[22] Further evidence for donation from the imido group into the $3b_2$ orbital is the lengthening of the Mo–C distances opposite the NR group. In the $3b_2$ orbital the interaction between the metal and these carbons is anti-bonding (Fig. 7). Thus strong π donor ligands can compete effectively with the cyclopentadienyl groups for the metal d orbitals, and consequently weaken metal–cyclopentadienyl bonding. It is found that the rings in such imido compounds are more readily displaced than in other metallocenes.

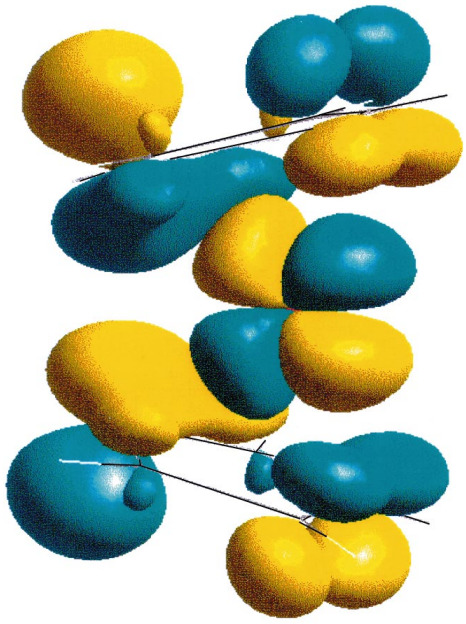

**Fig. 7** Iso-surface for the $3b_2$ orbital of a bent metallocene unit: the fourth frontier orbital

A similar bonding picture has been established for bis-cyclopentadienyl metal-oxo compounds.[23] The lack of cylindrical symmetry in the metallocene unit which provides only one effective π acceptor orbital for the oxo group leads to a build up of charge on the oxygen making it susceptible to electrophilic attack.

## 4 Some structural features of substituted metallocenes

Substitution of the hydrogens on a cyclopentadienyl group increases its size and can change its electron releasing properties.[12] It can also convey chirality on the complex to which it is bound.[24] The bulk of the substituents is important in determining the angle between the rings of a bent metallocene. Thus, for a fixed metal–ring distance, the larger the substituent the smaller the value of $\alpha$ needed to avoid steric interference between the groups. This is illustrated by the angles found for the tin metallocenes; $SnCp_2$ has $\alpha$ = 46°, $SnCp^*_2$ has $\alpha$ = 35.4° and $Sn(\eta\text{-}C_5Ph_5)_2$ has $\alpha$ = 0°. As with group 2 metallocenes the electronic preference for a bent structure appears to be marginal and the angle is controlled by the size of the substituent.

*ansa*-Metallocenes are those which have the two rings connected by a bridging group. Introduction of a bridge may constrain the geometry of the metallocene. A single atom bridge can increase $\alpha$ in comparison with the analogous compound with unbridged rings. Fig. 8 shows the angles $\gamma$ found for $MCp_2Cl_2$, where M = Ti, Zr and Hf, and for the analogues where the rings are bridged by $SiMe_2$ or $CMe_2$ groups.[25] The M–Cp centroid and M–Cl distances do not vary much from those of the parent metallocenes but the Si bridge reduces $\gamma$ by 0–4° and the C bridge by up to 10–13°. A single Si bridge has much the same effect as a two atom $C_2Me_4$ bridge. The metal tends to lie closer to the *ipso*-carbons and the two carbons adjacent to it than to the two opposite it, and the C–C bond opposite the *ipso*-carbons is shortened. When the rings are bent back by an *ansa*-bridge the coordination site at the metal is opened up and also the metal becomes more electrophilic.[25,26]

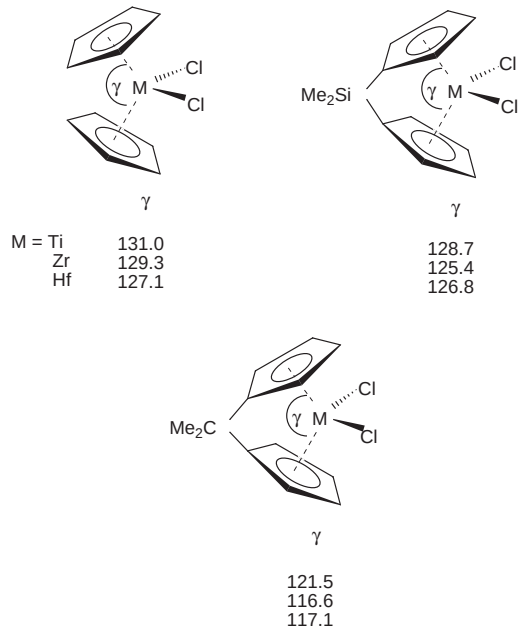


**Fig. 8** Cp(centroid)-metal-Cp(centroid) angles, $\gamma°$, found for a series of Group 4 metallocene dichlorides

The angles $\alpha$, $\beta$ and $\phi$ (Fig. 1b) are not given for these molecules, but in a series of *ansa*-bridged niobocene metallocenes with $CMe_2$ as the bridging group and similar $\gamma$ values, $\alpha$ values of 63–68° are found with $\phi$ values of 16–18°.[27] A comparison with *ansa*-bridged ferrocenes, also known as ferrocenophanes, which have a single Si bridge shows that $\varepsilon$ values are similar but, in contrast, the values for $\alpha$ lie around 20° and $\phi$ has a value of 37°. Because the $d^6$ ferrocene unit is much more reluctant to bend there is considerable strain energy in forming the *ansa*-ring and this is evidenced by the greater departure from planarity at the *ipso*-carbons.

## 5 Comments on selected reactions of metallocenes and their derivatives

The reactions described below are chosen to illustrate the role of the three co-planar orbitals and the interplay between orbital occupancy and inter-ring angle. In particular they focus on the differences between reactions of *ansa*-bridged metallocenes and the unbridged analogues.

### 5.1 Ring opening polymerisation of ferrocenophanes

The *ansa*-ring strain present in $d^6$ metallocenes has been utilised in forming ferrocene polymers.[28] For example heating [1]sila-ferrocenophane induces quantitative, exothermic ring opening polymerisation (ROP) [see (2)]. This ROP reaction may also be

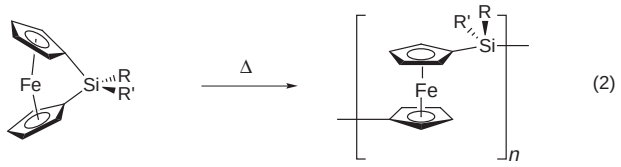


(2)

initiated at room temperature by using ionic initiators such as ferrocenyllithium followed by hydrolytic work-up (3). Early transition metal *ansa*-metallocenes are thermally stable and show no tendency to rupture the *ansa*-bridge. These differences in reactivity are consistent with the energy change of bending the various $d^n$ configurations discussed above.

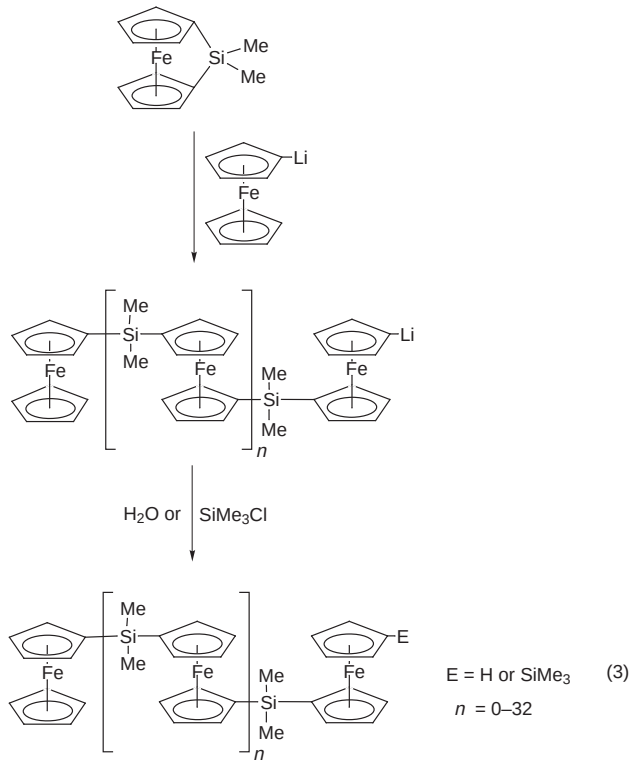


(3)

### 5.2 Elimination from $d^2$ metallocenes and addition to $d^4$ metallocenes

Brintzinger and co-workers[6,29] showed that whereas $MoCp_2(CO)$ and $WCp_2(CO)$ are thermally stable compounds formation of $CrCp_2(CO)$ is reversible. All three compounds had near identical CO stretching frequencies suggesting similar binding in the three CO complexes. The difference in reactivity was analysed by a combination of semi-empirical MO theory and ligand field theory and attributed to the repulsion between the d electrons that needs to be overcome on forming the CO complex. The metallocene has a triplet ground state with a configuration of $3a_1^2 2b_1^1 4a_1^1$. The CO complex is a singlet with a $d^4$ configuration $3a_1^2 2b_1^2$. Thus a promotion term is involved in the bond formation. The energy difference between the triplet ground state and the singlet excited state is greater for a first row metallocene, thus there is a bigger energy input in formation of $CrCp_2(CO)$ and conversely a greater energy gain on decomposition.

Significant reactivity differences are found between *ansa*-bridged and non *ansa*-bridged group 6 metallocene derivatives.[30] The dihydride $WCp_2H_2$ photochemically eliminates dihydrogen forming the triplet tungstenocene intermediate[13] which can, for example, insert into the C–H bonds of benzene [see (4)]. In contrast, the *ansa*-bridged analogue $W[(\eta^5\text{-}C_5H_4)_2CMe_2]H_2$ is photochemically inert.

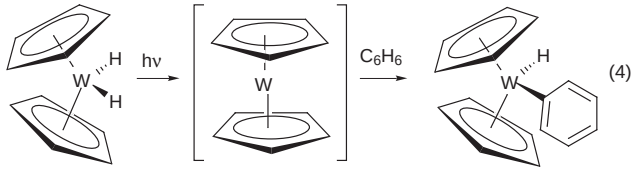


(4)

Similarly $WCp_2MeH$ thermally eliminates methane at 60 °C [see (5)] whereas $W[(\eta^5\text{-}C_5H_4)_2CMe_2]MeH$ is thermally stable at 110 °C.

The contrast between the two latter compounds is of particular interest as they both show intramolecular hydrogen exchange between the methyl group and the metal hydride. For $WCp_2MeH$ this hydrogen exchange is only marginally faster

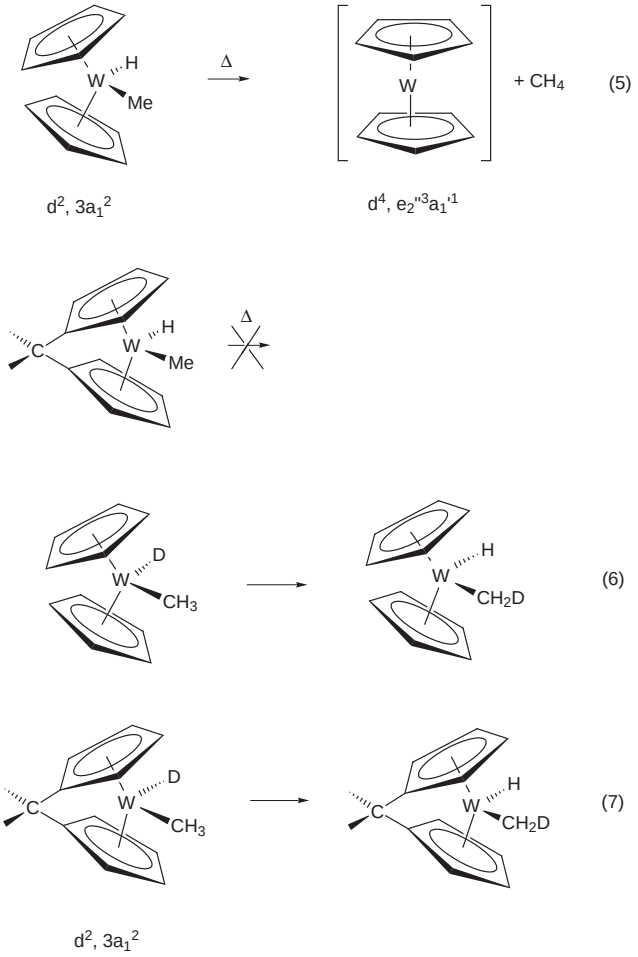


than the elimination reaction.[31] The exchange reactions pass through a mid-point in which a $CH_4$ moiety is bound to the

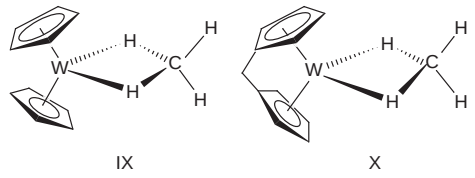


IX X

metal through two of its hydrogens, **IX** and **X**.[32] At this mid-point, the d configurations are $3a_1^2 2b_1^2$. The transition states for exchange are estimated to be of very similar energy. Elimination of methane from this mid-point is, however, calculated to be very different for the unbridged and *ansa*-bridged systems. The energy profiles for elimination are plotted in Fig. 9 as a function of W–C distance for a $C_{2v}$ system. The energy is referenced with respect to the methyl hydrides at zero. The mid-points for exchange, **IX** and **X**, are at the minima in the singlet energy curves. In both cases the tungstenocene product is expected to be in a triplet state. The unbridged compound has a close cross-over point to the triplet state and subsequent energy gain on forming triplet tungstenocene with parallel rings. In the *ansa*-bridged compound where the bridge prevents the rings achieving a parallel conformation, the singlet–triplet cross-over is at a greater metal–methane distance and is of higher energy. Also the eventual triplet product is of higher energy than the transition state for the exchange.

The driving force for reductive elimination in these Group 6 metallocene derivatives is seen to be the formation of the favoured parallel ring structure for the $d^4$ configuration metallocene product. When the rings are constrained by the

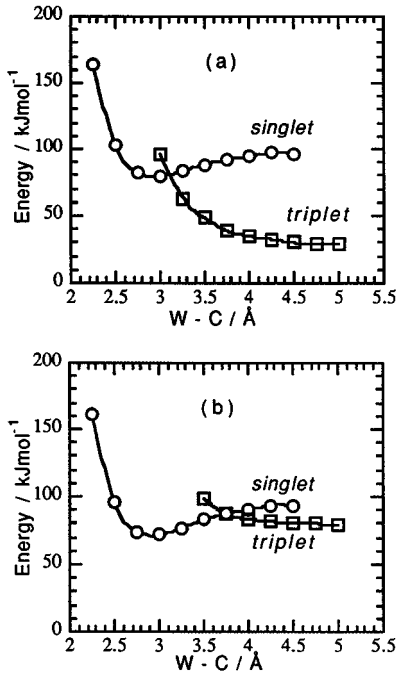


**Fig. 9** Energies of triplet and singlet $C_{2v}$ methane complexes (a) [W(η-$C_5H_5)_2(CH_4)$] and (b) [W((η-$C_5H_4)_2CH_2)(CH_4)$] at varying W–C distance with respect to the energy of the corresponding methyl hydride

*ansa*-bridge the four d electrons to avoid being spin paired have partially to occupy the high energy $4a_1$ orbital.

In the reactions of $d^0$ titanium metallocene derivatives Brintzinger has found that titanocene derivatives with an interannular ethylene bridge, while resembling the unbridged analogue in many transformations involving Ti(IV) or Ti(III) oxidation states, do not undergo reactions which are thought to involve a free titanocene Ti(II) intermediate.[33] Theoretical estimates of the energy difference between triplet titanocene with an $\alpha$ value of 50°, which is typical of that found in a Ti(IV) metallocene derivative, and the optimised $\alpha$ value of 26° is 0.63 eV or 60.78 kJ $mol^{-1}$. Such an energy gain, available to the unbridged titanocene, is not accessible if the inter-ring angle is constrained by an *ansa*-bridge; it may well account for the reactivity difference. For zirconocene the estimate is less, 0.21 eV or 20.26 kJ $mol^{-1}$. This, coupled with the greater difficulty in reducing Zr(IV) to Zr(II), means less striking differences are expected in the reactions of *ansa*-bridged and non-bridged zirconocene derivatives. The principal differences found appear to be associated with the increased electrophilicity of the metal associated with the presence of the *ansa*-bridge.[26]

### 5.3 Zeigler–Natta polymerisation catalysed by metallocene derivatives

Zirconocene dichloride in the presence of excess methylalumoxane (MAO) was found to catalyse the polymerisation of ethene to high density polypropylene.[9] Variation of the cyclopentadienyl groups has led to effective processes for both isotactic and syndiotactic polymerisation of propylene.[10,11,34] There is abundant evidence that the active species in these metallocene polymerisation catalysts are monomeric, cationic zirconocene alkyls, *e.g.* $[ZrCp_2R]^+$. The role of the MAO is to generate and stabilise the $d^0$ 14 electron cationic species.

The mechanism for Zeigler–Natta alkene polymerisation proposed by Cossée and Arlman[35] (8) involves a four centre transition state (8c) in which the new C–C bond is forming. If a methyl group and a coordinated ethene are brought close to one another steric repulsion between the hydrogens occurs before the carbon atoms are close enough to form an incipient bond. Brookhart and Green proposed a modification of the Cossée–Arlman mechanism in which the alkyl group tilted and formed

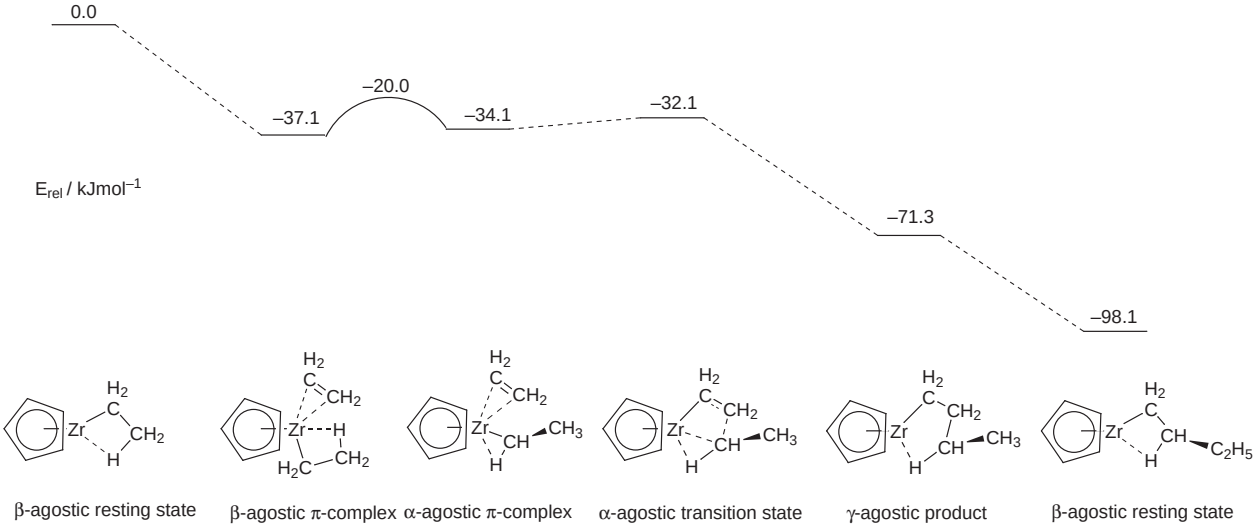


**Fig. 10** Key steps on the energy profile for insertion of ethene into the Zr–C bond of $[ZrCp_2Et]^+$ as calculated by Lohrenz *et al.*[38]

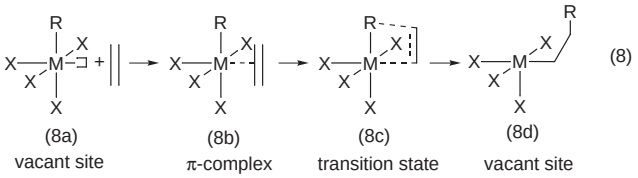


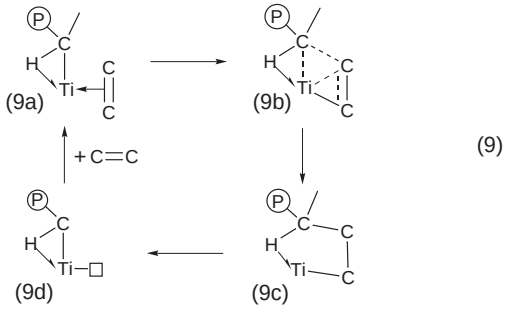


an $\alpha$-agostic hydrogen bond to the metal (9a).[36] Tilting of the methyl group relieves the steric hindrance betwen the alkyl and olefinic substituents in the transition state (9b). Formation of the agostic bond also provides an explanation for control of the stereochemistry of the polymerisation of propene since the substituents could lie either *cis*- or *trans*- with respect to the planar transition state.

Extensive experimental and theoretical investigations[37] have lent support to this picture of the reaction pathway. The results from one such theoretical study on the insertion of ethene into the metal–carbon bond of $[ZrCp_2C_2H_5]^+$ are summarised in Fig. 10.[38] The resting state of the process is calculated to be a β-agostic alkyl. The olefin binds to this exothermically. The alkyl chain then rotates to form an α-agostic π-complex which undergoes the insertion process resulting in a γ-agostic product which then returns to a β-agostic resting state.

Throughout the insertion reaction the key atoms, the alkyl α-carbon and α-agostic hydrogen, the two olefinic carbons and the metal all lie in the same plane. To enable such a reaction pathway, the metal must provide three co-planar orbitals, one to bind the olefin, one to form the metal–alkyl bond and one to form the agostic bond. Also the orbitals need to be sufficiently proximate for the C–C bond to form readily. The three frontier orbitals of a bent metallocene fulfill this role admirably.

The necessity for three available orbitals is underlined by the stability of the $d^2$ cation $[WCp_2(\eta^2\text{-}C_2H_4)Me]^+$. This cation fails to insert ethene into the W–C bond. Though the two d electrons will be involved in back-donation to the ethene resulting in stronger olefin binding than in a $d^0$ analogue, it is likely that the occupancy of the third orbital prevents the agostic bond formation needed to lower the activation energy barrier for the insertion step.

The history of metallocene chemistry is a classic example of the symbiosis of experiment and theory in its broadest sense. Synthetic ingenuity, detailed studies of mechanism and careful application of physical techniques have all played their part. In the future the relative availability and improved accuracy of modern computational methods should mean that they will also be useful tools to the synthetic chemist in planning experiments.

## 6 References


1 M. L. H. Green, *Organometallic Compounds*, 3rd edn., Methuen, London, 1968, vol. 2.
2 C. Balhausen and J. P. Dahl, *Acta Chem. Scand.*, 1961, **15**, 1333.
3 J. C. Green, M. L. H. Green and C. K. Prout, *J. Chem. Soc., Chem. Commun.*, 1972, 421.
4 J. C. Green, S. E. Jackson and B. Higginson, *J. Chem. Soc. Dalton Trans.*, 1975, 403.
5 J. L. Petersen and L. F. Dahl, *J. Am. Chem. Soc.*, 1975, **97**, 6416, 6422 and references therein.
6 H. H. Brintzinger, L. L. Lohr and K. L. Tang Wong, *J. Am. Chem. Soc.*, 1975, **97**, 5146.
7 J. W. Lauher and R. Hoffmann, *J. Am. Chem. Soc.*, 1976, **98**, 1729 and references therein.
8 M. L. H. Green, *Pure Appl. Chem.*, 1978, **50**, 27 and references therein.
9 A. Andersen, H.-G. Cordes, J. Herwig, W. Kaminsky, A. Merck, R. Mottweiler, J. Pein, H. Sinn and H.-J. Vollmer, *Angew. Chem., Int. Ed. Engl.*, 1976, **15**, 630.
10 J. A. Ewen, *J. Am. Chem. Soc.*, 1984, **106**, 6355.
11 W. Kaminsky, K. Külper, H. H. Brintzinger and F. R. W. P. Wild, *Angew. Chem., Int. Ed. Engl.*, 1985, **25**, 507.
12 M. L. Hays and T. P. Hanusa, *Adv. Organomet. Chem.*, 1996, **40**, 117.
13 P. Grebnik, R. Grinter and R. N. Perutz, *Chem. Soc. Rev.*, 1988, **17**, 453.
14 J. E. Bercaw, *J. Am. Chem. Soc.*, 1974, **96**, 5087.
15 A. J. Schultz, K. L. Stearley, J. M. Williams and R. Mink, *Inorg. Chem.*, 1977, **16**, 3303.
16 R. D. Wilson, T. F. Koettzle, D. W. Hart, Å. Kvick, D. L. Tipton and R. Bau, *J. Am. Chem. Soc.*, 1977, **99**, 1775.
17 D. M. Heinekey, *J. Am. Chem. Soc.*, 1991, **113**, 6074.
18 S. Camanyes, F. Maseras, M. Moreno, A. Ledós, J. M. Lluch and J. Bertrán, *J. Am. Chem. Soc.*, 1996, **118**, 4617 and references therein.

19 D. M. Heinekey, A. S. Hinkle and J. D. Close, *J. Am. Chem. Soc.*, 1996, **118**, 5353 and references therein.
20 G. Parkin and J. E. Bercaw, *J. Chem. Soc., Chem. Commun.* 1989, 255.
21 R. A. Henderson and K. E. Ogilvie, *J. Chem. Soc., Dalton Trans.*, 1993, 3431.
22 J. C. Green, M. L. H. Green, J. T. James, P. C. Konidaris, G. H. Maunder and P. Mountford, *J. Chem. Soc., Chem. Commun.*, 1992, 1361.
23 A. J. Bridgeman, L. Davis, S. J. Dixon, J. C. Green and I. N. Wright, *J. Chem. Soc., Dalton Trans.*, 1995, 1023.
24 R. L. Halterman, *Chem. Rev.*, 1992, **92**, 965.
25 R. M. Shaltout, J. Y. Corey and N. P. Rath, *J. Organomet. Chem.*, 1995, **503**, 205.
26 T. K. Woo, L. Fan and T. Ziegler, *Organometallics*, 1994, **13**, 2252.
27 N. J. Bailey, unpublished work.
28 I. Manners, *Adv. Organomet. Chem.*, 1995, **37**, 131.
29 K. L. Tang Wong and H. H. Brintzinger, *J. Am. Chem. Soc.*, 1975, **97**, 5143.
30 A. Chernega, J. Cook, M. L. H. Green, L. Labella, S. J. Simpson, J. Souter and A. H. H. Stephens, *J. Chem. Soc., Dalton Trans.*, 1997, 3225 and references therein.
31 R. M. Bullock, C. E. L. Headford, K. M. Hennessy, S. E. Kegley and J. R. Norton, *J. Am. Chem. Soc.*, 1989, **111**, 3897 and references therein.
32 J. C. Green and C. N. Jardine, *J. Chem. Soc., Dalton Trans.*, 1998, 1057.
33 J. A. Smith and H. H. Brintzinger, *J. Organomet. Chem.* 1981, **218**, 159.
34 J. A. Ewen, R. L. Jones, A. Razavi and J. D. Ferrara, *J. Am. Chem. Soc.*, 1988, **110**, 6255.
35 E. J. Arlman and P. Cossée, *J. Catal.*, 1964, **3**, 99 and references therein.
36 M. Brookhart and M. L. H. Green, *J. Organomet. Chem.*, 1983, **250**, 395.
37 R. H. Grubbs and G. W. Coates, *Acc. Chem. Res.*, 1996, **29**, 85 and references therein.
38 J. C. W. Lohrenz, T. K. Woo and T. Ziegler, *J. Am. Chem. Soc.*, 1995, **117**, 12793 and references therein.

*Received 12th January 1998*
*Accepted 6th April 1998*